DE GRUYTER OPEN

Acta Geophysica
vol. 63, no. 4, Aug. 2015, pp. 957-977
DOI: 10.1515/acgeo-2015-0034

Surface Deformation due to Loading of a Layered Elastic Half-space: Constructing the Solution for a General Polygonal Load

Michael BEVIS[1], Ernian PAN[2], Hao ZHOU[1], Feng HAN[2], and Richard ZHU[2]

[1]School of Earth Sciences, Ohio State University, Columbus, Ohio, USA
e-mail: mbevis@osu.edu

[2]Department of Civil Engineering, University of Akron, Akron, Ohio, USA

Abstract

We describe an algorithm for rapidly computing the surface displacements induced by a general polygonal load on a layered, isotropic, elastic half-space. The arbitrary surface pressure field is discretized using a large number, n, of equally-sized circular loading elements. The problem is to compute the displacement at a large number, m, of points (or stations) distributed over the surface. The essence of our technique is to reorganize all but a computationally insignificant part of this calculation into an equivalent problem: compute the displacements due to a single circular loading element at a total of $m\,n$ stations (where $m\,n$ is the product $m \times n$). We solve this "parallel" problem at high computational speed by utilizing the sparse evaluation and massive interpolation (SEMI) method. Because the product $m\,n$ that arises in our parallel problem is normally very large, we take maximum possible advantage of the acceleration achieved by the SEMI algorithm.

Key words: surface loading, elastic response, isotropic, layered half-space.

1. INTRODUCTION

The elastic response to surface loading has interested mathematicians, scientists and engineers for more than a century (Boussinesq 1885, Lamb 1901, Terazawa 1916, Love 1929). Interest in this topic within the Earth sciences has rapidly expanded in the last decade, following the widespread recognition that geodetic measurements can be used to observe oscillations of the Earth's surface that are driven by seasonal changes in the mass loads imposed on the solid Earth by the atmosphere, the hydrosphere and the cryosphere (Heki 2001, Blewitt *et al.* 2001, Van Dam *et al.* 2001, Dong *et al.* 2002). The elastic response to these environmental loading cycles is developed at global (Blewitt *et al.* 2001), regional (Heki 2001, Davis *et al.* 2004, Bevis *et al.* 2012) and local scales (Bevis *et al.* 2004, 2005). The near-field response to concentrated loads is influenced by shallow elastic structure which is highly variable in continental crust, particularly in the vertical direction (Bevis *et al.* 2004, 2005; Mooney *et al.* 1998). The layered, elastic half-space provides a useful mathematical framework for modeling Earth's instantaneous response to loading cycles when these loads are imposed over apertures which are small compared to the radius of the planet. The emerging use of continuous GPS networks to sense changes in ice mass within active ice sheets (*e.g.*, Hager 1991, Khan *et al.* 2007, Bevis *et al.* 2009, 2012) constitutes an important class of application.

Typically, the Earth's elastic response to changing surface loads of regional extent is computed using spectral methods (*e.g.*, Sasgen *et al.* 2005) and a global Earth structure model such as PREM (Dziewonski and Anderson 1981). The vertical resolution of whole Earth models like PREM is limited, especially near the surface. Indeed, PREM does not distinguish between the oceans and continents, let alone account for the rapid vertical variations in elastic moduli that frequently occur in the upper few kilometers of continental crust (Mooney *et al.* 1998). Bevis *et al.* (2004, 2005) argued that the near-field response to surface load changes is sensitive to the details of shallow elastic structure. This sensitivity could complicate (at least locally) the agenda of using crustal motion geodesy to gauge ice mass changes. We will illustrate this possibility by considering the elastic rebound associated with ice mass changes in Greenland. It is easier to include thin crustal layers in the Cartesian framework of Pan *et al.* (2007) (and this paper) than it is to do so in a spectral model implemented for a spherical Earth, since the latter approach would require harmonic expansions of very high degree to achieve the necessary radial resolution.

This paper is the sequel to the paper by Pan *et al.* (2007), in which we developed a precise numerical solution for the surface displacements produced by a uniform circular load imposed on the surface of a layered, elastic

half-space. This solution is computationally expensive, and so we also developed the sparse evaluation and massive interpolation (SEMI) method, which provides an approximate solution for the displacement field at very large numbers of points with vastly less computation per point (Pan *et al.* 2007). This approach utilizes the symmetry of the problem and the fact that the radial and vertical components of surface displacement are functions only of the radial distance, r, from the center of the load. We use our high accuracy but computationally expensive method to compute the displacement vectors at a limited number of r values (called control points or knots), and then use a variety of fast interpolation methods to determine the displacements at much larger numbers of intervening points. We can trade off the computational leverage achieved with the SEMI method and the magnitude of the errors associated with its approximations by choosing to use fewer or greater numbers of knots. The computational advantage of the SEMI method increases with the ratio of the number of surface stations to the number of knots.

In this paper we show how a circular loading element can be used to compute the surface displacement fields for an arbitrary surface load. Suppose we wish to compute the displacement at n stations due to a load we will approximate with m circular loading elements. The essence of our technique is to reorganize all but a computationally insignificant part of this calculation into an equivalent problem: compute the displacements due to a single circular loading element at a total of $m\,n$ stations (where $m\,n$ is the product $m \times n$). This maximizes the ratio of the number of stations to the number of knots, and so takes maximum possible advantage of the SEMI algorithm.

After describing this method in detail, we present some basic numerical tests of our code. In particular we address the problem of determining an appropriate number of loading elements for approximating a given load. Here the goal is to control the amplitude of artifacts or errors associated with discretization of the load. Lastly we consider some example loading problems and show how depth controlled variations in the elasticity constants can cause interesting and diagnostic features in surface displacement fields. These examples indicate that measuring the spatial development of the elastic response to known patterns of surface loading will enable us to infer information about subsurface structure. Of course, inversions of this kind require the forward problem to be evaluated many times, and it is this requirement which prompted us to develop a computationally efficient means for solving the forward problem for non-trivial loading geometries.

Before launching into this agenda, we note the following elementary points: (i) that the great advantage of using circular loads rather than point loads is that point loads produce displacement singularities and circular

loads do not; (ii) we use circular loading cells rather than finite loading cells of some other shape because circles are axi-symmetric, as is the layered material that we invoke; and (iii) all linear systems allow for superposition, and since we invoke a linear elastic material, then we can compute the response to multiple loading cells by superposing the solutions obtained for each individual loading cell. It is the axi-symmetric nature of the loading element problem, plus our ability to invoke superposition, that allows us to reframe the original problem into the parallel problem, and thereby achieve a large computational acceleration.

2. PROBLEM STATEMENT

Following Pan *et al.* (2007), we consider a layered half-space made up of p parallel, elastic, isotropic layers lying over an elastic, isotropic half-space. We adopt a Cartesian coordinate system in which the x and y axes lie in the surface plane ($z = 0$), and the z axis is positive downwards into the half-space. We assume that the surface of this half-space is subject to an imposed pressure field within a polygonal boundary B. The pressure P is zero everywhere outside of B, and is a known function $P(x, y)$ within and on B. The pressure P can be identified with the normal stress component σ_{zz}, and P is taken to be positive if the associated force is directed in the positive z direction. We assume that no shear tractions are imposed on the surface.

We wish to represent the pressure field within B using a suite of simple loading elements or cells, with the surface pressure applied within a single element being laterally uniform. The pressure field $P(x, y)$ is most easily approximated as piecewise constant by dividing the polygon into a regular grid of square loading cells (Fig. 1a), and assuming that the pressure everywhere within the i-th square cell is $\overline{P}_i = P(x_i, y_i)$, where (x_i, y_i) are the coordinates of the point in the center of that cell. There are two weaknesses to this approach: (i) the outer edges of the suite of square loading cells do not exactly correspond to the geometry of the polygon (Fig. 1a), and (ii) the actual pressure field $P(x, y)$ is not piecewise constant, and so the net force imposed by the pressure field on any square may deviate from that implied by the piecewise constant representation described above. However, by refining the grid so as to reduce the size of the individual cells, the errors associated with these problems can be reduced until they are negligible.

We cannot, in fact, use square loading cells, because square loads lack the symmetry which is essential to the SEMI method. We must use circular loading cells instead. However, it is useful to consider the circular loading cells as representing the square cells discussed above. Let us assume that the square cells in Fig. 1a had a width of $2a$, in which case the corresponding circular cells have radius a, as seen in Fig. 1b. Let us suppose that the i-th

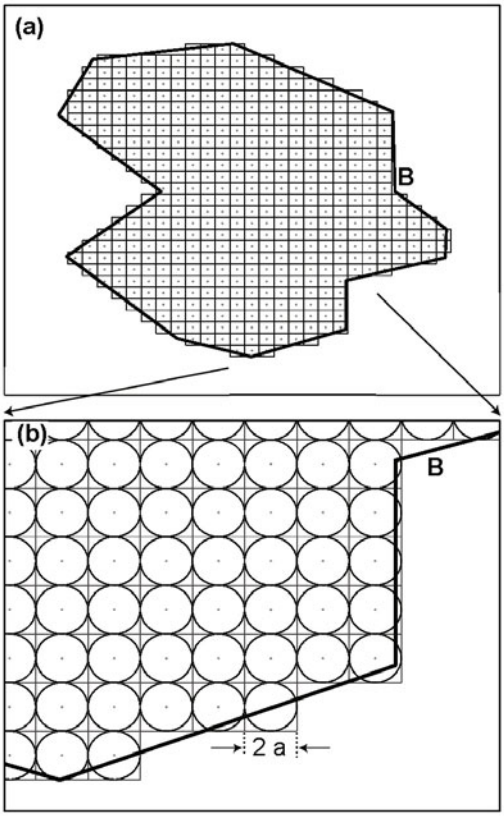

Fig. 1. Discretization of a surface pressure field $P(x,y)$ applied within a polygonal boundary B: (a) a square grid is developed for the loading area, and the average pressure in each square cell is approximated by the pressure at the center of that cell; (b) the load imposed within each square loading cell will actually be represented by a uniform circular load of diameter 2a, which nominally exerts the same net force as the square load.

circle lies within the *i*-th square, so both are centered at point (x_i, y_i). The area of the square is $A_s = 4a^2$, and that of the circle is $A_c = \pi a^2$. Clearly the use of a circular loading element is problematic because it cannot properly tile or cover the entire polygon – there are gaps between adjacent circles (Fig. 1b). However, we can largely overcome this problem by appropriate choice of the pressure we will assign to each circular element. If the constant pressure applied in the *i*-th circular cell is Q_i, and this load is to produce the same total force on the surface as the constant pressure $\overline{P}_i$ applied within the square cell, then we require $A_c Q_i = A_s \overline{P}_i$. So we should set

$$Q_i = \frac{4}{\pi} P\left(x_i, y_i\right) . \tag{1}$$

We have scaled the actual pressure at the center of each circular loading element by an amount that accounts for the gaps between the circles. There are still some minor problems associated with this piecewise constant but discontinuous representation of the original pressure field, as we will discuss in Section 4, but by making the circular elements sufficiently small, we can reduce the magnitude of these problems to any level that we desire.

We can now state our problem, assuming that the decomposition of the load into circular loading elements has already been achieved: given a multi-layered elastic half-space described using the notation of Pan *et al.* (2007), and given a set of n circular loads with the same radius (a) but different pressures (Q_i, for $i = 1, 2, ..., n$), compute the displacements at m stations located on the surface of the half-space.

3. DESCRIPTION OF THE ALGORITHM

In this section we describe the algorithm used to solve the problem just stated. Before developing this algorithm in a form suitable for efficient coding of the general problem, we explain the essence of our approach by considering an extremely simple example involving just two circular loads, 1 and 2, and a single station, S (Fig. 2). The pressure applied in the first circle is Q_1, and that in the second circle is Q_2. By linear superposition we can

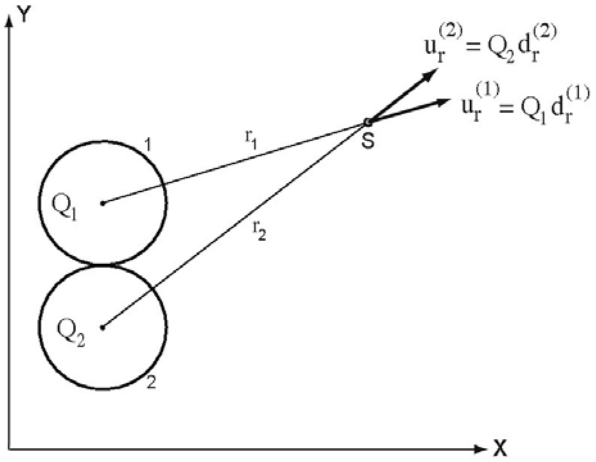

Fig. 2. The horizontal displacements induced at station S by uniform circular pressure loads Q_1 and Q_2. These problem geometry including the displacement field can be expressed in radial coordinate systems attached to the center of each load, and in a global Cartesian coordinate system {X, Y}.

state that the displacement vector **u** at S is the vector sum of the displacements $\mathbf{u}^{(1)}$ and $\mathbf{u}^{(2)}$ due to the first and second loads, respectively. Given the symmetry of a single circular load, the displacement it causes at any station is most easily described and computed in a cylindrical coordinate system whose origin lies at the center of the load. In this coordinate system, the displacement vector at any point has only two non-zero components – the vertical component u_z and the radial component u_r. Because each load has its own cylindrical coordinate system, we must transform vectors $\mathbf{u}^{(1)}$ and $\mathbf{u}^{(2)}$ into Cartesian coordinates in order to perform the vector summation and deliver the solution **u** in the same coordinate system in which the load and station geometry are described. Let us represent this coordinate transformation in standard matrix form $\mathbf{u}_{\text{cart}} = \mathbf{T}\,\mathbf{u}_{\text{cyl}}$. (Because the matrix **T** is sparse in this particular context, this is not the most efficient way in which to implement the transformation. We ignore this minor detail for now). We choose not to compute $\mathbf{u}^{(1)}$ and $\mathbf{u}^{(2)}$ explicitly, but instead compute $\mathbf{d}^{(1)}$ and $\mathbf{d}^{(2)}$ which are the displacement vectors at S produced by unit pressure loading of our circular loading domains. Let us assume that $\mathbf{d}^{(1)}$ and $\mathbf{d}^{(2)}$ are computed and expressed in cylindrical (or local) coordinate systems attached to each load, and that we wish to express the net displacement **u** at S in the Cartesian (or global) coordinate system. Then

$$\mathbf{u} = Q_1\mathbf{T}^{(1)}\mathbf{d}^{(1)} + Q_2\mathbf{T}^{(2)}\mathbf{d}^{(2)} \quad , \tag{2}$$

where $\mathbf{T}^{(1)}$ is the transformation matrix associated with load 1, *etc*. There are two important points about this equation. Firstly, almost all of the computational burden involved in evaluating this equation is incurred in evaluating $\mathbf{d}^{(1)}$ and $\mathbf{d}^{(2)}$. The coordinate transformations and the summation are computationally trivial in comparison. Secondly, when considered from the perspective of their local coordinate systems the two unit loads are identical, and since the spatial variability of the surface displacement field **d** depends only on r (since the symmetry of the load implies no θ dependence), then $\mathbf{d}^{(1)} = \mathbf{d}(r_1)$ and $\mathbf{d}^{(2)} = \mathbf{d}(r_2)$, and we can view the evaluation of **d** as solving the problem of two stations and a single unit load, rather than two unit loads and a single station.

This second insight is the crucial one. If we want to compute the displacement at a single station due to m circular loads, we can do most of the work by solving the parallel problem of determining the displacements caused at m stations by a single unit circular load. In the original problem r_i is the distance between the station and the center of the i-th unit circular load. In the parallel problem, r_i is the distance between the center of the single unit circular load and the i-th station. Having solved this parallel problem we can construct the solution to the original problem by the obvious general-

ization of Eq. 2. We can extend this trick even further: the problem of solving the displacements at m surface stations due to n circular loads (with common radius a) can be very largely transformed into the problem of finding the displacements at $n\,m$ stations due to a single unit circular load. The great advantage of diverting to the parallel form of the problem is that the computational efficiency of the SEMI method increases in proportion with the total number of stations.

We are ready now to present the algorithm for the problem stated in its most general form. We wish to compute the displacements at m stations due to n circular loads. Each of these loads has identical radius a. The i-th circular load is centered at (x_i^c, y_i^c) and is subject to uniform pressure Q_i, which is considered positive if the associated force is oriented in the z-direction, *i.e.*, into the half-space. The j-th station has surface coordinates (x_j^s, y_j^s). Consider the k-th combination of the i-th circle and the j-th station (Fig. 3). We can consider k the station number in the parallel problem. The relative position vector describing the position of station j relative to circle i is

$$\mathbf{r}^k = \mathbf{r}^{ij} = \left(x_j^s - x_i^c\right)\hat{\mathbf{x}} + \left(y_j^s - y_i^c\right)\hat{\mathbf{y}} \tag{3}$$

which has Euclidean length

$$r^k = r^{ij} = \sqrt{\left(x_j^s - x_i^c\right)^2 + \left(y_j^s - y_i^c\right)^2} \tag{4}$$

which is simply the distance from the center of load i to station j in the original problem, or the distance from the center of the single unit load to the k-th station in the parallel problem. The unit vector which points from the center of circle i to station j is

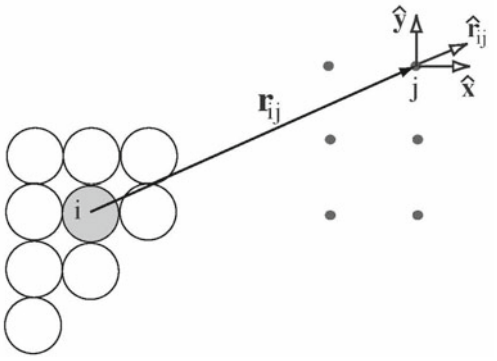

Fig. 3. The coordinate systems used to describe the horizontal displacement at station j due to load i.

$$\hat{\mathbf{r}}^{ij} = \hat{r}_x^{ij}\hat{\mathbf{x}} + \hat{r}_y^{ij}\hat{\mathbf{y}} \tag{5}$$

where

$$\hat{r}_x^{ij} = \frac{\left(x_j^s - x_i^c\right)}{r^{ij}} \ , \quad \hat{r}_y^{ij} = \frac{\left(y_j^s - y_i^c\right)}{r^{ij}} \ . \tag{6}$$

We use the SEMI method (Pan *et al.* 2007) to solve for the parallel problem, finding a total of $m\,n$ displacement vectors

$$\mathbf{d}^k = d_r^k\hat{\mathbf{r}} + d_z^k\hat{\mathbf{z}} \ \equiv d_r^{ij}\hat{\mathbf{r}} + d_z^{ij}\hat{\mathbf{z}} \tag{7}$$

produced by the single unit circular load. In order to revert to our original problem we must transform these vectors into the global Cartesian coordinate system, *i.e.*, find

$$\mathbf{d}^{ij} = d_x^{ij}\hat{\mathbf{x}} + d_y^{ij}\hat{\mathbf{y}} + d_z^{ij}\hat{\mathbf{z}} \tag{8}$$

for $i = 1, 2, .., n$ and $j = 1, 2, ..., m$, or, equivalently, for $k = 1, 2, \ldots, n\,m$. The vertical (z) component has the same value in local and global coordinates. We need only to transform the horizontal vector components. This can be done by projecting the radial component of **d** onto unit vectors in the X and Y directions (Fig. 3), *i.e.*

$$d_x^{ij} = d_r^{ij}\ \hat{r}_x^{ij} \ , \quad d_y^{ij} = d_r^{ij}\ \hat{r}_y^{ij} \ . \tag{9}$$

We can now express the displacement at each station due to a unit load at the position of the n non-unit loads in the original problem. To solve the displacement at a given station (j) in response to the original n circular loads, we simply scale the unit load responses (Eq. 8) with the appropriate loads, *i.e.*

$$\mathbf{u}^j = \sum_{i=1,n} Q_i\mathbf{d}^{ij} \ . \tag{10}$$

4. SOME NUMERICAL TESTS AND EXAMPLES

We begin with a test in which we attempt to reproduce the solution presented by Becker and Bevis (2004) for a uniform rectangular load on a uniform elastic half-space (UHS), which is known as Love's Problem. We do this using our SEMI approach by invoking a layered elastic half-space (LHS), consisting of 3 layers on a half-space, in which all four of these layers have identical elastic properties – the general problem thus degenerates into the special case (UHS), and the solutions should match.

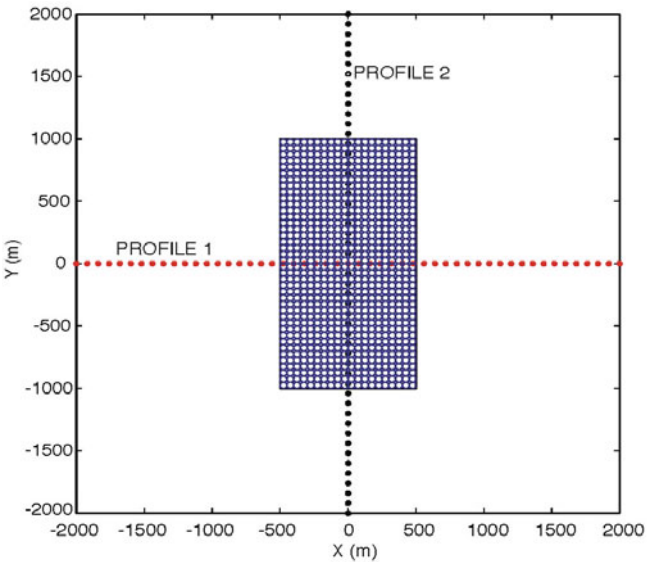

Fig. 4. A uniform rectangular load is approximated by an array of circular loading elements, and the resulting surface displacement field is sampled along profiles 1 and 2.

The geometry associated with this problem is shown in Fig. 4. The 1 km $\times 2$ km rectangle is an idealized representation of a lake, and the pressure loading corresponds to a water depth of 100 m. We evaluate the surface displacement field along two profiles (1 and 2) each of which bisect the load. We follow the notation of Becker and Bevis (2004) in which the x, y, and z components of displacement are called u, v, and w, respectively. We evaluate the UHS solution assuming that Young's modulus $E = 0.6 \times 10^{11}$ Nm^{-2} and Poisson's ratio $\nu = 0.25$ (or, equivalently, that the Lamé parameters λ and μ are given by $\lambda = \mu = 2.4 \times 10^{10}$ Nm^{-2}). We set surface pressure $P = \rho g h$ where $\rho = 1000$ kg m^{-3}, $g = 9.82$ ms^{-2} and $h = 100$ m. These exact solutions are shown by the red dots in Fig. 5. In order to test our SEMI code, we approximate the load using $20 \times 40 = 800$ circular loading elements (Fig. 4) and invoke a LHS in which the first three layers have thicknesses of 1500, 3000, and 6000 m, and the fourth layer is semi-infinite. We set $E = 0.6 \times 10^{11}$ Nm^{-2} and $\nu = 0.25$ in all four layers. The resulting solution is shown by the blue curves in Fig. 5. We can see that the UHS and LHS correspond very closely for all points (or stations) outside of the rectangle, and closely within the rectangle. A careful examination shows that within the rectangle the SEMI solution for the degenerate LHS oscillates around the exact solution for the UHS.

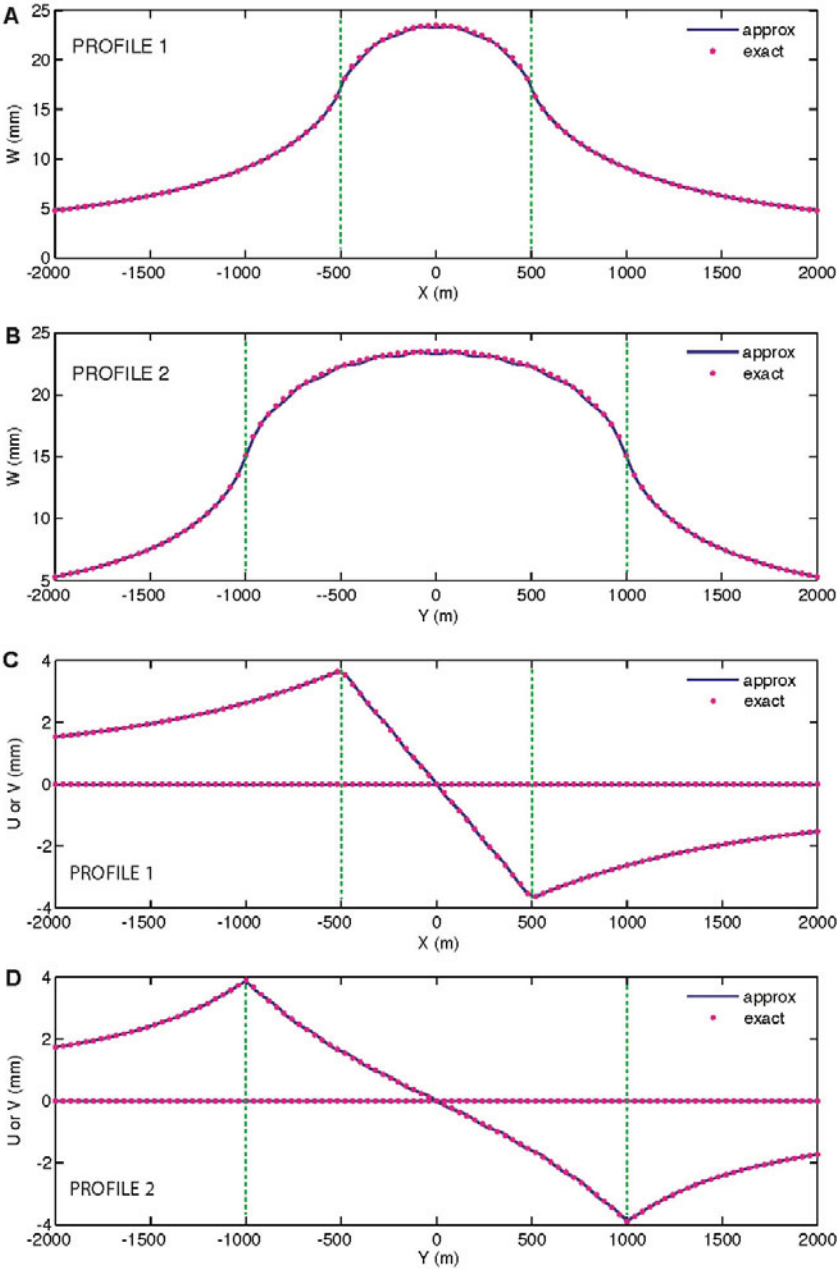

Fig. 5. The horizontal (u and v) and vertical (w) components of displacement along each profile (see Fig. 4) computed exactly using the equations of Becker and Bevis (2004), and using the approximation techniques developed in this paper. The dotted green lines indicate the edges of the rectangular load.

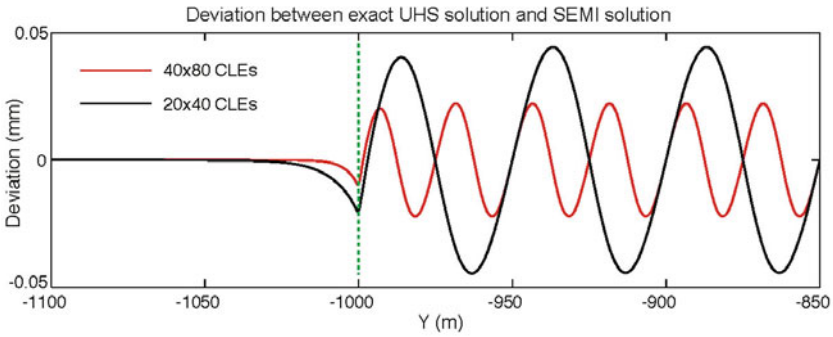

Fig. 6. The deviation between the exact and the SEMI solutions for the vertical displacements near the edge of the rectangle (see Fig. 4) for two cases in which the load is approximated by: (i) a 20 × 40 array, and (ii) a 40 × 80 array of circular loading elements.

This oscillatory behavior, which we call ripple, is made more obvious in Fig. 6 in which we difference the two sets of solutions for the horizontal component of displacement, u, along a small segment of profile 2, where it crosses the bottom side of the rectangle. The black curve shows the difference between the solutions when the load is approximated by $20 \times 40 = 800$ circles (corresponding to the SEMI solution shown in Fig. 5). This oscillation has a sinusoidal or "egg crate" form within the rectangle, and wavelength of this sinusoid (in the x and y directions) is the distance ($2a$) between the centers of adjacent circular loading elements (CLEs). Clearly the ripple in the SEMI solution manifests the discretization of the load using CLEs. The red curve shows the SEMI solution error or ripple when $40 \times 80 = 3200$ CLEs are used. Halving the radius of the CLE reduces the wavelength and the amplitude of the ripple by a factor of two (Fig. 6), at the cost of increasing the computational burden by a factor of 4. But since the SEMI algorithm is so fast, it will usually be possible to reduce the magnitude of ripple to an acceptable level at an acceptable computational cost.

We now consider some examples which test the SEMI algorithm in the context of a non-degenerate LHS (*i.e.*, the layers have different elastic constants) by developing certain special or limiting cases in which our intuition provides us with an expected outcome or value. In both of the examples that follow we consider the surface response to a single uniform circular load of radius a. This load is applied to an elastic space consisting of one layer of thickness t overlying a half-space. It is often more instructive to refer to the normalized layer thickness, $T = t/a$. We shall assume that Poisson's ratio, ν, is 0.25 for both layers, and that Young's modulus is E_1 in the upper layer, and E_2 in the underlying half-space. Because of the symmetry of the circular

load, the surface displacement vector at each point has only vertical and radial components, and both are purely a function of r, the radial distance from the center of the load. In plotting this dependence we shall use the normalized radial distance, r/a. We contrast the surface response for this 2-layer space with the surface response of a UHS subject to the same load, assuming that this UHS has $\nu = 0.25$ and Young's modulus equal either to E_1 or to E_2.

We first consider the problem of a thick layer on a half-space, for which $t >> a$, or $T >> 1$. This geometry is shown in the left hand part of the diagram (comprising two vertical sections) inset into Fig. 7a. We assume that $E_1 = 0.1$, $E_2 = 1$ and consider two values for the thickness of the upper layer: $T = 10$ and $T = 100$. The vertical and radial displacement profiles are shown in Fig. 7a, b, respectively, and can be compared to the UHS response for the case in which Young's modulus $E_{UHS} = E_1 = 0.1$. By comparing these response curves we can confirm what we might have guessed intuitively: if the upper layer of the 2-layer space is very much thicker than radius of the load, the surface response in the near and medium field of the load is almost identical to that of a UHS whose properties are those of the upper layer.

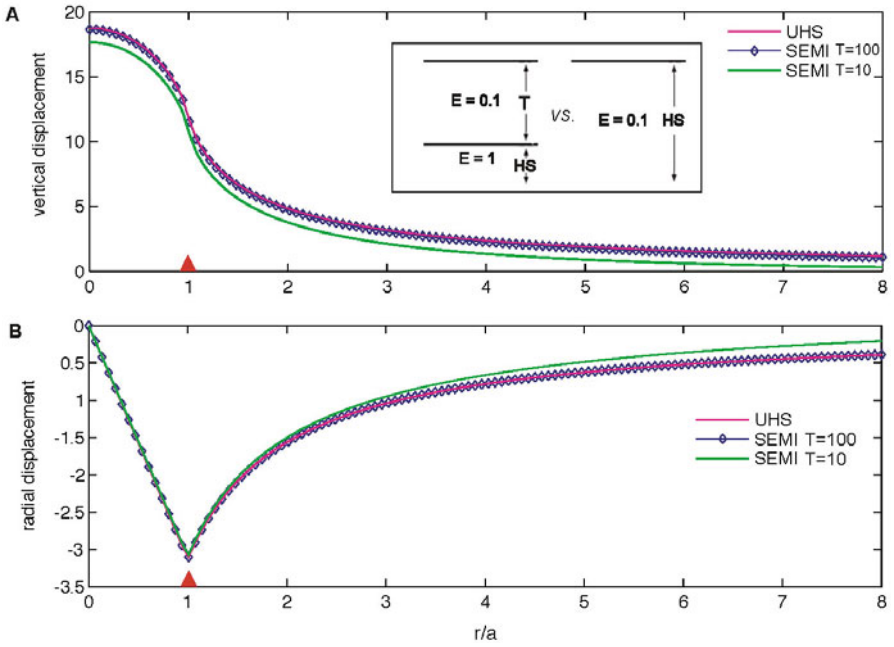

Fig. 7. A comparison between the: (a) vertical, and (b) radial displacements caused by a uniform circular load imposed on: (i) a uniform half-space (UHS) with $E = 0.1$, and (ii) a layer of thickness t and $E = 0.1$ overlying a half-space with $E = 1.0$, as depicted in the inset in sub-plot (a). The comparison between the UHS and 2-layer solutions are presented for $T = t/a = 10$ and $T = 100$.

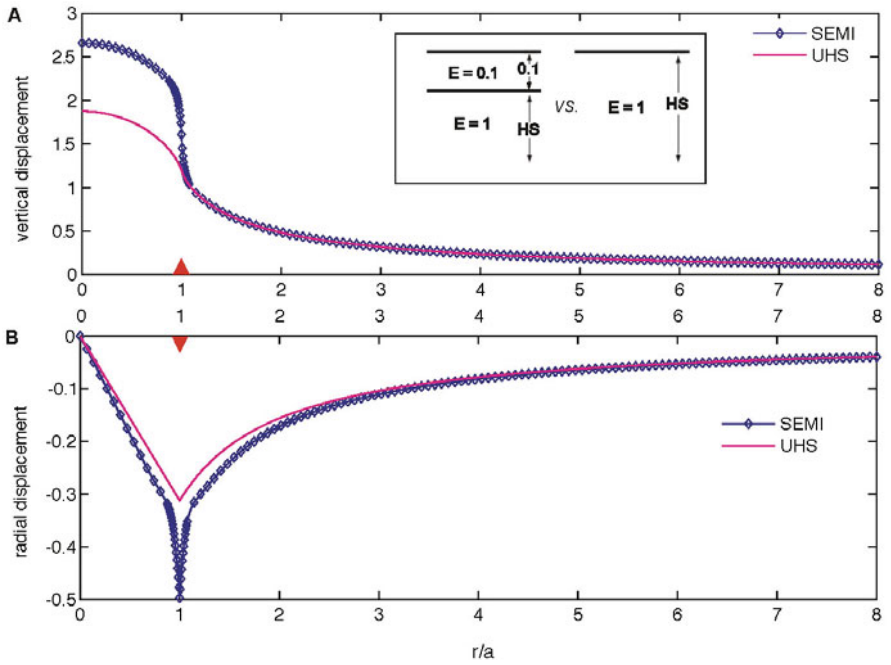

Fig. 8. A comparison between the: (a) vertical, and (b) radial displacements caused by a uniform circular load imposed on: (i) a uniform half-space with $E = 1.0$, and (ii) a layer of thickness $t = 0.1\,a$ and $E = 0.1$ overlying a half-space with $E = 1.0$, as depicted in the inset in sub-plot (a).

Next we consider the "opposite" problem from that just discussed, in which the first layer of the 2-layered space is much "thinner" than the radius of the circular load (specifically $T = 0.1$). In this case one might suspect that the influence of the thin upper layer would be restricted, and so it is useful to compare this response to the UHS response in which $E_{\mathrm{UHS}} = E_2 = 1$. Comparing these response profiles we see that the vertical surface displacement profiles are very distinct within the loading domain. Since the LHS has a very compliant upper layer, the surface beneath the load is deflected to a much greater extent than in the case of the UHS (Fig. 8a). But for $r > a$, the vertical response of the LHS is very nearly identical to that of the UHS. In other words, the surface response of the layered space is strongly influenced by the first layer within the loading area, but is dominated by the lower layer a short distance outside of the load. If we examine the radial component of displacement for this same problem (Fig. 8b) we see that in the medium field (say $r > 3a$) the surface response of the LHS is dominated by the lower layer (it matches the response of a UHS with the same properties as the 2nd layer of the LHS). The LHS and UHS responses differ to their

greatest extent at the boundary of the circle ($r = a$). As we can see from the UHS response curve, the load tends to pull material near the edge of the circle inwards as well as downwards. In the case of the LHS the very compliant upper layer leads to an enhanced inwards displacement, and the width of the "spike" in the LHS response curve is influenced by the thickness of the first layer.

Lastly we consider the accuracy of the SEMI algorithm itself, in the primitive context of evaluating the displacements due to a single circular load of unit radius. Here the question is how accurate is the approximation delivered by the SEMI method in comparison with (much slower) direct evaluation? We investigated this issue by generating a suite of elastic structure models using a Monte Carlo approach. We generated 50 models consisting of five layers over a half-space, and 50 models consisting of 9 layers over a half-space. Each layer thickness was generated randomly, and within our ensemble thicknesses ranged between 0.070 and 8282 m. Young's modulus and Poisson's ratio for each layer were also randomly generated, with the former falling in the range 0.11-5147 Nm^{-2}, and the later in the range 0.01-0.49. In every case the load had a radius of 1 m, and the surface displacement field was evaluated at 1250 stations from $r = 0$ to $r = 1000$ m, with more than half of the stations falling in the range 0-40 m. For each subsurface model the vertical and horizontal displacement components we computed directly and using the SEMI approach, these quantities were compared. This amounted to a total of 125 000 comparisons for each component of displacement. We defined the "relative error" as the difference between the SEMI and the directly computed value for displacement divided by the directly computed value. The RMS relative errors were 5.1×10^{-3} for the radial component and 3.1×10^{-3} for the vertical component. This result was obtained using our standard SEMI code which employs a total of 134 knots.

It should be kept in mind that when we model a general surface load using many circular loading elements, the interpolation errors associated with the different loading elements will tend to cancel at a specific station, particularly in the near field of the load where the displacements are largest.

5. WEIGHING THE ICE SHEETS WITH GPS: THE IMPACT OF SHALLOW GEOLOGICAL STRUCTURE

We now use our computer code to implement a more substantial and interesting calculation. We wish to demonstrate that including thin, near-surface layers of compliant sedimentary rock layers into our Earth model can produce significant changes to the computed response for a given loading or unloading scenario. We will illustrate this possibility by considering the

solid Earth's elastic adjustment to ice load changes in Greenland. Our goal here is not so much to compute the best possible model for such a response, but rather to show that the fine details of near-surface elastic structure can actually make a difference to Earth's response to typical (*i.e.*, realistic) changes in ice mass. That is, our purpose here is to perform a sensitivity study.

We use the ice loss grids of Krabill *et al.* (2000) that represent the spatial pattern of ice surface height changes (dH/dt) in Greenland during the interval 1995-2000. We chose this grid because it covers all of Greenland in a consistent way. We consulted with Bill Krabill and Bob Thomas to establish estimates of the near surface densities (depending on surface elevation) that allow us to convert height rates (dH/dt) to mass rates (dM/dt). We are well aware that the rate of ice loss in Greenland has accelerated quite dramatically since the year 2000. So our ice mass rate (dM/dt) grid represents something of a baseline measurement. Nevertheless, this calculation will serve to illustrate the potential impact of shallow geological structure on the Earth's unloading response. We approximated the surface loading field (dM/dt) using 7178 disk loads for the purpose of computing Earth's elastic response.

We use the crustal structure model CRUST 2.0 (http://igppweb.ucsd.edu/~gabi/crust2.html) to provide a reasonable estimate for the average crustal structure beneath Greenland. CRUST 2.0 provides a layered model for the crust and uppermost mantle, in each 2° by 2° square, specifying both the P and S wave velocity for each layer, as well as density. Given these three parameters it is a simple matter to estimate the two elastic parameters for each layer – either the two Lamé parameters, or, equivalently, Young's modulus (E) and Poisson's ratio (ν). We averaged the results we obtained over most of Greenland and adopted this nominal structure for the purpose of modeling the Earth's elastic response to changing ice loads. We combined this average CRUST 2.0 structure for the crust and upper mantle (above 400 km depth) with the PREM structure for the deeper Earth (below 400 km depth) – we refer to this as the HYBRID elastic structure model. Whereas our discretized version of PREM has a top layer 3 km thick composed of a material with $E = 68$ GPa and $\nu = 0.28$, the top layer in HYBRID is only 359 m thick and has $E = 8.17$ GPa and $\nu = 0.35$.

CRUST 2.0 identifies several areas in coastal Greenland in which the near-surface compliant layer is 1 km thick rather than just 359 m thick. This is basically an intelligent guess based on local surface geology. We have produced a third elastic structure model, called HYBRID/S, by modifying HYBRID so that its first (presumably sedimentary) layer is 1 km thick. We used our computer code to compute the vertical velocity of the Earth's crust in response to the ice mass rate field derived from Krabill *et al.* (2000), using the PREM, HYBRID, and HYBRID/S models for elastic structure. The re-

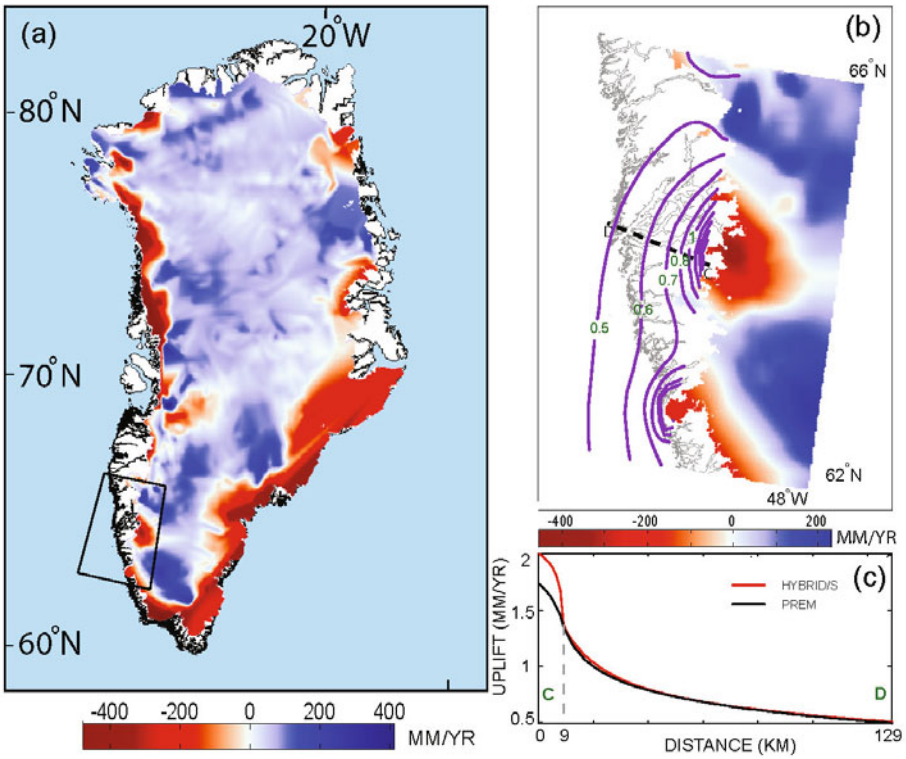

Fig. 9: (a) The average rate of ice surface elevation change in the time interval 1995-2000, according to Krabill *et al.* (2000). This height rate field (dH/dt) was converted into a mass rate field (dM/dt), in order to compute the Earth's elastic response to load changes. (b) A blow up, depicting part of SW Greenland, showing vertical crustal velocity contours adjacent to the ice sheet, and the location of the velocity profile D-C. The contours are those predicted using PREM structure. (c) The elastic rebound velocities along the profile D-C are predicted using the structure models PREM and HYBRID/S. The last model invokes a 1 km thick layer of relatively compliant rocks (presumably sediments) immediately beneath the surface of the crust, as suggested by model CRUST 2.0. The dashed vertical line represents the ice front. Note that when we use HYBRID/S rather than PREM, the rate of elastic rebound coincident with the load is increased by about 10%. This figure is modified from Zhou (2008).

bound velocities predicted using PREM and HYBRID are everywhere similar (differences are less than a few percent), but the results obtained using HYBRID/S are quite distinct in the near-field of the zones of major ice loss (Fig. 9). This finding indicates, not surprisingly, that a near-surface layer of relatively low stiffness enhances the rate of elastic rebound within and immediately adjacent to the changing load.

Whereas it is reasonable to use global Earth structure models such as PREM to model the medium- and far-field elastic response to surface loading or unloading, and even much of what is considered the near-field, this choice of structure model will usually cause the very-near-field loading response to be underestimated, since PREM does not resolve the strong near-surface decline in stiffness characteristic of many continental areas. While lateral heterogeneity of shallow elastic structure may be something of a complication for space geodetic studies of ice mass balance, it might also be something of an opportunity in that an unusually compliant shallow subsurface regime might act as an "amplifier" of the vertical crustal motion signals produced by local ice loss.

6. DISCUSSION

Approximating a spatially finite but otherwise general pattern of surface loading with a suite of circular loading elements (of equal diameter) allows us to exploit the computational acceleration associated with the SEMI method presented in Pan *et al.* (2007). This paper builds on their results and utilizes their computer codes. In turn, Pan *et al.* (2007) was motivated by the application and the algorithm presented here. The key idea discussed here is the reformulation of all but a computationally minor component of the problem of finding the displacements at m stations due to n circular loads into the "parallel" problem of computing the displacement produced at $n\,m$ stations in response to a single circular load. This is precisely the problem that the SEMI method was designed to address. Note, however, that the problem reformulation presented herein is in no way tied to the specific interpolation strategies employed by a code that implements the SEMI algorithm for a single circular load. Our code for computing the displacement field due to a suite of circular loading elements calls a distinct code that implements the SEMI method for solving the "primitive" or elementary problem of a single circular load. This modularity makes it easy to incorporate any improvements that may be achieved in the SEMI method.

The methodology described in this paper is very simple to state and to implement. We have stated the algorithm in great, and perhaps a surprising level of detail. This is because the whole point of this paper, and Paper 1, is computing a solution as rapidly as possible. It would be easy to present our algorithm using equations that are more compact and/or more evocative than those used above, and yet do so in a way that potentially wastes computer time. We have avoided the use of the transformation matrix $\mathbf{T}$ that appears in Eq. 2, for example, because 4 of its 9 elements are zero and we do not want to waste time computing products and sums that contribute nothing towards the final solution. Similarly we have avoided computing trigonometric or in-

verse trigonometric functions. At the risk of appearing pedantic, we have presented the computation in what seems to us a nearly optimal approach for coding the algorithm.

The computational acceleration associated with the strategy presented here, combining problem reformulation and the SEMI method, is particularly useful in solving inverse problems, since inverse methods often involve solving the forward problem thousands or even hundreds of thousands of times. Having solved the inverse problem using the approach described in this paper, one could use the direct method described in Paper 1, to explore the solution in more detail, for example by evaluating quantities, such as the subsurface strain field, that did not feature in the inverse problem. Perhaps the most serious drawback of the SEMI method is that it is restricted to computing fields at the surface of the half-space.

Acknowledgements. MB and HZ were supported by NASA contract NNG04GF28G and NSF grant ARC-1111882. EP, FH, and RZ were partially supported by the Ohio DOT.

References

Becker, J.M., and M. Bevis (2004), Love's problem, *Geophys. J. Int.* **156**, 2, 171-178, DOI: 10.1111/j.1365-246X.2003.02150.x.

Bevis, M., E. Kendrick, A. Cser, and R. Smalley Jr. (2004), Geodetic measurement of the local elastic response to the changing mass of water in Lago Laja, Chile, *Phys. Earth Planet. In.* **141**, 2, 71-78, DOI: 10.1016/j.pepi.2003.05.001.

Bevis, M., D. Alsdorf, E. Kendrick, L.P. Fortes, B. Forsberg, R. Smalley Jr., and J. Becker (2005), Seasonal fluctuations in the mass of the Amazon River system and Earth's elastic response, *Geophys. Res. Lett.* **32**, 16, L16308, DOI: 10.1029/2005GL023491.

Bevis, M., E. Kendrick, R. Smalley Jr., I. Dalziel, D. Caccamise, I. Sasgen, M. Helsen, F.W. Taylor, H. Zhou, A. Brown, D. Raleigh, M. Willis, T. Wilson, and S. Konfal (2009), Geodetic measurements of vertical crustal velocity in West Antarctica and the implications for ice mass balance, *Geochem. Geophys. Geosyst*. **10**, 10, Q01005, DOI: 10.1029/2009GC002642.

Bevis, M., J. Wahr, S.A. Khan, F.B. Madsen, A. Brown, M. Willis, E. Kendrick, P. Knudsen, J.E. Box, T. van Dam, D.J. Caccamise II, B. Johns, T. Nylen, R. Abbott, S. White, J. Miner, R. Forsberg, H. Zhou, J. Wang, T. Wilson, D. Bromwich, and O. Francis (2012), Bedrock displacements in Greenland manifest ice mass variations, climate cycles and climate change, *Proc. Natl. Acad. Sci. USA* **109**, 30, 11944-11948, DOI: 10.1073/pnas.1204664109.

Blewitt, G., D. Lavallée, P. Clarke, and K. Nurutdinov (2001), A new global mode of Earth deformation: Seasonal cycle detected, *Science* **294**, 5550, 2342-2345, DOI: 10.1126/science.1065328.

Boussinesq, J.V. (1885), *Application des Potentiels à l'Etude de l'Equilibre et du Mouvement des Solides Elastiques*, Gauthier-Villars, Paris, 508 pp. (in French).

Davis, J.L., P. Elósegui, J.X. Mitrovica, and M.E. Tamisiea (2004), Climate-driven deformation of the solid Earth from GRACE and GPS, *Geophys. Res. Lett*. **31**, 24, L24605, DOI: 10.1029/2004GL021435.

Dong, D., P. Fang, Y. Bock, M.K. Cheng, and S. Miyazaki (2002), Anatomy of apparent seasonal variations from GPS-derived site position time series, *J. Geophys. Res*. **107**, B4, 2075, DOI: 10.1029/2001JB000573.

Dziewonski, A.M., and D.L. Anderson (1981), Preliminary reference Earth model, *Phys. Earth Planet. In*. **25**, 4, 297-356, DOI: 10.1016/0031-9201(81) 90046-7.

Hager, B.H. (1991), Weighing the ice sheets using space geodesy: A way to measure changes in ice sheet mass, *EOS Trans. AGU* **72**, 17, 91.

Heki, K. (2001), Seasonal modulation of interseismic strain buildup in northeastern Japan driven by snow loads, *Science* **293**, 5527, 89-92, DOI: 10.1126/ science.1061056.

Khan, S.A., J. Wahr, L.A. Stearns, G.S. Hamilton, T. van Dam, K.M. Larson, and O. Francis (2007), Elastic uplift in southeast Greenland due to rapid ice mass loss, *Geophys. Res. Lett.* **34**, 21, L21701, DOI: 10.1029/2007 GL031468.

Krabill, W., W. Abdalati, E. Frederick, S. Manizade, C. Martin, J. Sonntag, R. Swift, R. Thomas, W. Wright, and J. Yungel (2000), Greenland ice sheet: High-elevation balance and peripheral thinning, *Science* **289**, 5478, 428-430, DOI: 10.1126/science.289.5478.428.

Lamb, H. (1901), On Boussinesq's problem, *Proc. Lond. Math. Soc*. **34**, 1, 276-284, DOI: 10.1112/plms/s1-34.1.276.

Love, A.E.H. (1929), The stress produced in a semi-infinite solid by pressure on part of the boundary, *Philos. Trans. Roy. Soc. Lond. A* **228**, 377-420, DOI: 10.1098/rsta.1929.0009.

Mooney, W.D., G. Laske, and T.G. Masters (1998), CRUST 5.1: A global crustal model at 5° × 5°, *J. Geophys. Res*. **103**, B1, 727-747, DOI: 10.1029/ 97JB02122.

Pan, E., M. Bevis, F. Han, H. Zhou, and R. Zhu (2007), Surface deformation due to loading of a layered elastic half-space: A rapid numerical kernel based on a circular loading element, *Geophys. J. Int.* **171**, 1, 11-24, DOI: 10.1111/ j.1365-246X.2007.03518.x.

Sasgen, I., D. Wolf, Z. Marinec, V. Klemann, and J. Hagerdorn (2005), Geodetic signatures of glacial changes in Antarctica: Rates of geoid height change

and radial displacement due to present and past ice-mass variations, GFZ Scientific Technical Rep. STR05/01, GeoForschungsZentrum, Potsdam, Germany.

Terazawa, K. (1916), On the elastic equilibrium of a semi-infinite solid under given boundary conditions, with some applications, *J. Coll. Sci. Imp. Univ. Tokyo* **37**, 7, 1-64.

van Dam, T., J. Wahr, P.C.D. Milly, A.B. Shmakin, G. Blewitt, D. Lavallée, and K.M. Larson (2001), Crustal displacements due to continental water loading, *Geophys. Res. Lett*. **28**, 4, 651-654, DOI: 10.1029/2000GL012120.

Zhou, H. (2008), Layered Cartesian half-space models for Earth's elastic response to contemporary surface loading phenomena, Ph.D. Thesis, Ohio State University, Columbus, USA, 160 pp.

Received 14 March 2014
Received in revised form 28 October 2014
Accepted 29 October 2014